

STRUCTURE OF $^{70,72}\text{Ge}$ NUCLEI POPULATED IN $^{12,13}\text{C} + ^{64}\text{Ni}$ REACTIONS

George DRAFTA¹, Sorin PASCU², Dan PANTELICĂ³, Gheorghe CĂTA-DANIL⁴

În această lucrare au fost investigate experimental câteva din canalele mai puțin favorizate ale reacțiilor nucleare $^{12}\text{C} + ^{64}\text{Ni}$ și $^{13}\text{C} + ^{64}\text{Ni}$ și anume: $^{64}\text{Ni}(^{12}\text{C}, \alpha 2n\gamma)^{70}\text{Ge}$, $^{64}\text{Ni}(^{12}\text{C}, \alpha\gamma)^{70}\text{Ge}$, $^{64}\text{Ni}(^{13}\text{C}, \alpha 3n\gamma)^{70}\text{Ge}$ și $^{64}\text{Ni}(^{13}\text{C}, \alpha n\gamma)^{72}\text{Ge}$. S-a reușit confirmarea unor date existente deja în literatură, precum și măsurarea rapoartelor DCO pentru mai multe tranziții gama în nucleele $^{70,72}\text{Ge}$. Au fost efectuate calcule în cadrul modelului IBA-1 și rezultatele au fost comparate cu datele experimentale existente.

In this paper we investigated experimentally some of the less favored channels of the $^{12}\text{C} + ^{64}\text{Ni}$ and $^{13}\text{C} + ^{64}\text{Ni}$ nuclear reactions, namely $^{64}\text{Ni}(^{12}\text{C}, \alpha 2n\gamma)^{70}\text{Ge}$, $^{64}\text{Ni}(^{12}\text{C}, \alpha\gamma)^{70}\text{Ge}$, $^{64}\text{Ni}(^{13}\text{C}, \alpha 3n\gamma)^{70}\text{Ge}$, and $^{64}\text{Ni}(^{13}\text{C}, \alpha n\gamma)^{72}\text{Ge}$. The results confirm the data already existing in the literature. We also measured DCO ratios for several gamma transitions in $^{70,72}\text{Ge}$ nuclei. Calculations were performed within the IBA-1 model framework, and the results were compared with available experimental data.

Key words: nuclear structure, $^{70,72}\text{Ge}$, in-beam γ -ray spectroscopy, IBA-1 model

1. Introduction

Investigation of the $A \sim 70$ mass region has turned out many interesting results. The $2p_{1/2}$, $1f_{5/2}$, $2p_{3/2}$ and $1g_{9/2}$ orbitals are determinant for the structure of this region. Calculations of the equilibrium configurations based on the configuration-dependent shell-correction approach with deformed Woods-Saxon potentials [1] predict competing stabilizing gaps at both positive and negative quadrupole deformations. Rapidly changing nuclear properties (such as shape) are seen for small variations in neutron or proton number, spin and excitation energy

¹ PhD, Horia Hulubei National Institute of Physics and Nuclear Engineering, DFN, Măgurele, C.P. MG-6, R-077125, Romania, e-mail: drafta@tandem.nipne.ro

² PhD, Horia Hulubei National Institute of Physics and Nuclear Engineering, DFN, Măgurele, C.P. MG-6, R-077125, Romania

³ PhD, Horia Hulubei National Institute of Physics and Nuclear Engineering, DFN, Măgurele, C.P. MG-6, R-077125, Romania

⁴ Prof. Physics Department, University POLITEHNICA of Bucharest and National Institute for Physics and Nuclear Engineering “Horia Hulubei”, Măgurele, Romania

[2]. Other unusual features can be found, of which strong collectivity, large quadrupole deformations (up to $\beta \approx 0.4$), and shape coexistence at low energy and spin are but a few examples [3,4]. For instance, when varying the neutron number of the even-even Ge isotopes one notices a non-regular dependence of the excitation energy of the first excited 0_2^+ state [5-10].

Prior to 2010, there were only a few experiments of in-beam γ -ray spectroscopy on medium- and high-spin states of ^{70}Ge using heavy ions and fusion-evaporation reactions (however, different methods such as Coulomb excitation were employed [7-10]). A couple of experiments were undertaken more than three decades ago [11,12] and a more recent one [13] in 2000, with more modern methods and detectors that brought new information on high spin states up to spin (21), but nothing new on medium spin states. Very recently, the medium spin states of ^{70}Ge were investigated [14] and the level scheme was partly modified. The most recent compilation of data pertaining ^{70}Ge is reported in [15].

The most recent in-beam γ -ray spectroscopy experimental study aimed at investigating the high spin structure of ^{72}Ge was performed in 1979 [19] using the $^{70}\text{Zn}(\alpha, 2n\gamma)^{72}\text{Ge}$ reaction, and the latest compilation of available data on this nucleus obtained using a variety of methods is reported in [20].

A variety of theoretical approaches have been employed in an attempt to reproduce the available data, including the boson expansion techniques [16], the interacting boson model [17], the Hartree-Fock-Bogoliubov method with the quantum number projection [18] and the shell model [14].

In this paper we intend to investigate the low and medium spin structure of ^{70}Ge and ^{72}Ge using the $^{64}\text{Ni}(^{12,13}\text{C},\text{evap})^{70,72}\text{Ge}$ reaction, by means of in-beam γ -ray spectroscopy techniques and compare the results with theoretical calculations based on the Interacting Boson Approximation (IBA-1).

2. Experimental method and data analysis

The experiment was performed at the recently modernized 9 MV Van de Graaff Tandem accelerator of IFIN-HH [21]. In-beam γ -ray spectroscopy was performed on the reaction products obtained through bombarding a thick ($\sim 65\mu\text{m}$), self supported target of enriched ^{64}Ni foil with ^{12}C at 40 MeV and ^{13}C at 45 MeV.

The radiations produced in these reactions were detected by an array of particle, γ - and X-ray detectors. A ring of five large volume high purity germanium (HPGe) detectors was placed at 143° backwards, one HPGe gamma detector and one planar X-ray detector were set at 90° and 270° , respectively, one HPGe gamma detector was placed at 37° forward, and one neutron detector was set at 321.5° forward. All angles are measured with respect to the beam direction. Four fast response $\text{LaBr}_3:\text{Ce}$ detectors with typical energy resolution of 2-3% at

662 keV and time resolution between 100 and 300 ps (depending on the crystal size) were also used for timing purposes, as well as one particle detector inside the reaction chamber.

In this paper we investigate some of the less favored reaction channels, namely those that yield ^{70}Ge and ^{72}Ge . While the target was enriched in ^{64}Ni , traces of isotopes found in natural Ni (i.e. $^{58,60,61,62}\text{Ni}$) could still be found in the foil. The most abundant isotopes in naturally occurring nickel are ^{58}Ni with 68.27% and ^{60}Ni with 26.10%. ^{61}Ni and ^{62}Ni can be found in more modest proportions of 1.13% and 3.59%, respectively, while ^{64}Ni is the scarcest of all at 0.91%.

Cross-section calculations were performed using the codes CASCADE [22] and PACE IV (part of the LISE++ software package [23]) and it was found that for a 40 MeV incident energy ^{12}C projectile producing ^{70}Ge the highest value is for $^{61}\text{Ni}(^{12}\text{C}, 2p\gamma)^{70}\text{Ge}$ ($\sigma = 194.38$ mb), while for $^{60}\text{Ni}(^{12}\text{C}, 2p\gamma)^{70}\text{Ge}$ is $\sigma = 151.7$ mb. For the main component of the target, $^{64}\text{Ni}(^{12}\text{C}, \alpha 2n\gamma)^{70}\text{Ge}$, we still have $\sigma = 60.78$ mb. The highest cross section for ^{72}Ge comes from the interaction with ^{62}Ni and is $\sigma = 21.95$ mb. The rest of them are insignificant or zero.

For a ^{13}C projectile at 45 MeV incident energy the cross-section for $^{64}\text{Ni}(^{13}\text{C}, \alpha\gamma)^{72}\text{Ge}$ is $\sigma = 23.7$ mb, and for $^{64}\text{Ni}(^{13}\text{C}, \alpha 3n\gamma)^{70}\text{Ge}$ is $\sigma = 0.973$ mb. Significant cross section for the producing of ^{70}Ge are yielded by the interaction of $^{61,62}\text{Ni}$ with ^{13}C (149 mb and 85.2 mb, respectively), while the production of ^{72}Ge from ^{62}Ni is more modest ($\sigma = 38.6$ mb).

List-mode data acquisition yielded almost 300 GB of data during the seven days of the experiment. Calibration as well as activation spectra were taken to ensure proper identification of the transitions of interest and the contaminants. Data were sorted off-line in 2-D coincidence matrices ($\gamma\text{-}\gamma$, *particle* $\text{-}\gamma$, etc) and 3-D coincidence cubes ($\gamma\text{-}\gamma\text{-}\gamma$, $\gamma\text{-}\gamma\text{-particle}$, etc.), and projection spectra were obtained and analyzed using GASPWare software package [24].

An efficiency curve of the experimental set-up was obtained using a ^{152}Eu source and subsequently used for efficiency correction of the transition intensities observed in the spectra.

Due to the fact that these are non-dominant channels, we do not expect to see all but the strongest transitions in the projection spectra. Also, in fusion-evaporation reactions with heavy ions the populated states are mostly the yrast ones, so this is another limitation that must be taken into account. Gates were placed on the strongest known transitions in ^{70}Ge and ^{72}Ge , allowing us to see coincident transitions.

For ^{72}Ge was chosen a gate on the lowest yrast transition (the $2_1^+ \rightarrow 0_1^+$, 834 keV transition, originating on the first 2^+ excited state, and ending up on the ground state). We were able to see most of the known yrast cascade up to spin

10^+ at 4820 keV, part of the negative parity band cascade up to spin 11^- at 5838 keV, and other transitions.

Unfortunately we were not able to use the $4_1^+ \rightarrow 2_1^+$, 894 keV transition in the yrast cascade due to contamination with a transition of the same energy from another nucleus.

In ^{70}Ge the situation is more complicated: both $2_1^+ \rightarrow 0_1^+$ and the $10_1^+ \rightarrow 8_1^+$ transitions in the yrast cascade have the same energy (1039 keV), therefore a gate on 1039 keV would yield false intensities for the yrast cascade transitions. So we selected the second lowest yrast transition, corresponding to the $4_1^+ \rightarrow 2_1^+$, 1113 keV de-excitation of ^{70}Ge .

Here, we were able to see the yrast cascade up to the 10^+ , 5243 keV level and part of the negative parity band cascade up to the 7^- , 3955 keV level.

A spectrum gated on the $2_1^+ \rightarrow 0_1^+$, 834 keV transition from ^{13}C on ^{64}Ni reaction and one gated on the $4_1^+ \rightarrow 2_1^+$, 1113 keV transition from ^{12}C on ^{64}Ni are

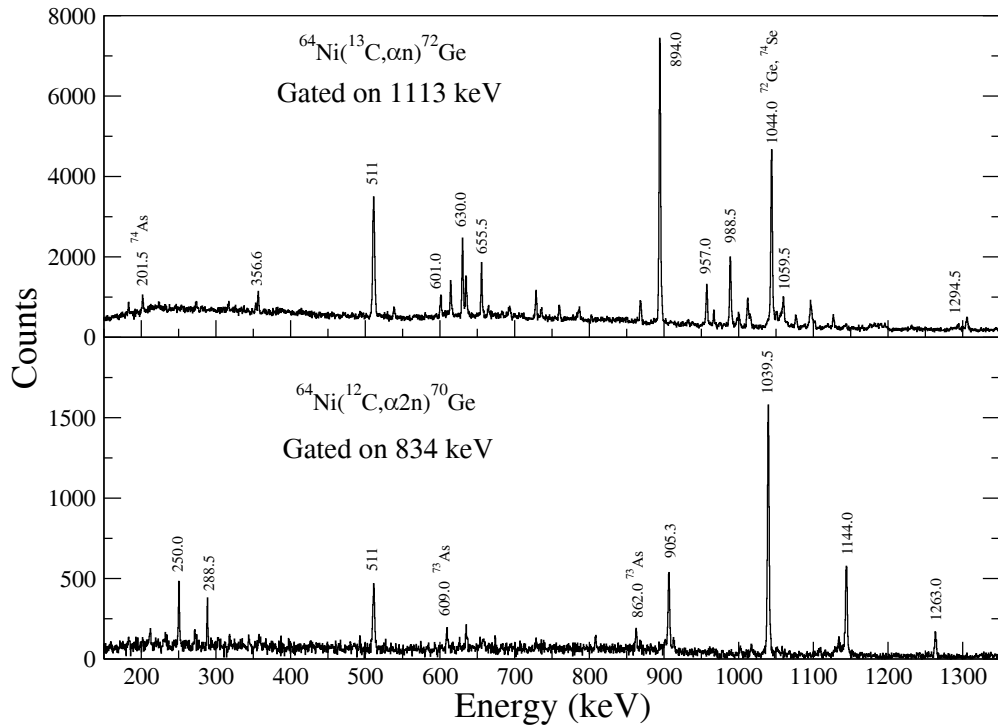


Fig. 1 Gated spectra on the $2_1^+ \rightarrow 0_1^+$ 834 keV transition from ^{13}C on ^{64}Ni reaction and $4_1^+ \rightarrow 2_1^+$ 1113 keV transition from ^{12}C on ^{64}Ni . See text for details.

3. IBA – 1 Calculations and Comparison with Experimental Values

The calculations were performed in the IBA-1 framework (no distinction made between protons and neutrons) using the Extended Consistent Q-formalism (ECQF) [25]. The Hamiltonian employed was [26]:

$$\begin{aligned} \hat{H}_{sd} = \varepsilon \hat{n}_d + \kappa (\hat{Q} \cdot \hat{Q})^{(0)} + a_3 & \left[(\hat{d}^+ \tilde{d})^{(3)} \times (\hat{d}^+ \tilde{d})^{(3)} \right]^{(0)} \\ & + a_4 \left[(\hat{d}^+ \tilde{d})^{(4)} \times (\hat{d}^+ \tilde{d})^{(4)} \right]^{(0)} \end{aligned} \quad (1)$$

where \hat{Q} is the quadrupole operator given by :

$$\hat{Q} = [(\hat{s}^+ \tilde{d}) + (\hat{d}^+ \tilde{s})] + \chi (\hat{d}^+ \tilde{d})^{(2)}$$

and $\varepsilon, \kappa, \chi, a_3$ and a_4 are the model parameters. Second quantization notation is used: \hat{s}^+ and \hat{d}^+ are the creation operators for spin zero and spin two bosons, respectively, while \tilde{s} and \tilde{d} are the annihilation operators for the same bosons.

The electromagnetic transition operators are:

$$\begin{aligned} \hat{T}(E2) &= e_2 \hat{Q} \\ \hat{T}(M1) &= \alpha [\hat{Q} \times \hat{L}]^{(1)} + \beta \hat{L} \end{aligned}$$

where e_2 represents the boson effective charge and α and β are other parameters [26]. The Hamiltonian was numerically diagonalized with the code PHINT [27]. The electromagnetic decay rates were calculated with the code FBEM [27].

The three dynamical symmetries of the IBA are given by the competition between the five parameters ($\varepsilon, \kappa, \chi$, OCT and HEX) of the Hamiltonian of Eq. (1). The ε/κ ratio reflects the competition between the spherical-driving term ($\varepsilon \hat{n}_d$) and the deformation inducing term ($\hat{Q} \cdot \hat{Q}$). χ specifies the degree of γ -softness, from axially symmetric [SU(3)] to γ -soft [O(6)] nuclei. The other two parameters do not mix the basis states and provides only a specific diagonal contribution.

The quantities that represent key observables for the structure of collective even-even nuclei were taken into account in the present fits: $R_{4/2} = E(4_1^+)/E(2_1^+)$, $R_{0/2} = E(0_2^+)/E(2_1^+)$ and $R_{\gamma/2} = E(2_\gamma^+)/E(2_1^+)$ energy ratios, the absolute values of the electromagnetic transition probabilities (in W.u.), and the $R_{2\gamma} = B(E2; 2_\gamma^+ \rightarrow 0_1^+)/B(E2; 2_\gamma^+ \rightarrow 2_1^+)$ branching ratio. All the parameters from the Hamiltonian were determined in order to reproduce these collective

observables. The effective charge, e_2 , was determined by normalizing the predictions to the experimental $B(E2; 2_1^+ \rightarrow 0_1^+)$ value from ^{70}Ge .

The numerical values used for the model parameters are given in Table 1.

Table 1
Numerical values of model parameters used in ^{70}Ge and ^{72}Ge calculations

Parameter	^{70}Ge	^{72}Ge
ε [MeV]	1.69	1.47
κ [MeV]	-0.025	-0.022
χ	-0.49	-0.29
a_3 [MeV]	0.33	0.24
a_4 [MeV]	-0.56	-0.53
e_2 [eb]	0.06	0.06
α [μ_N]	0.006	0.003
β [μ_N]	0.05	0.05

In Fig. 2 we present a comparison of theoretical values based on our calculations and known experimental data in ^{70}Ge : excitation energies and reduced electric quadrupole transition probabilities for low-lying, positive parity levels.

In Fig. 3 we present a similar comparison of theoretical values based on our calculations and known experimental data in ^{72}Ge .

The properties of the ground state band (energies and $B(E2)$ s) and those of the quasi- γ band are well described for both nuclei. The energy of the first excited 0^+ state could not be reproduced by the calculations, confirming the intruder character of these states in ^{70}Ge and ^{72}Ge . However, the distribution in energy for the low-energy 0^+ states agrees rather well with the experimental observations.

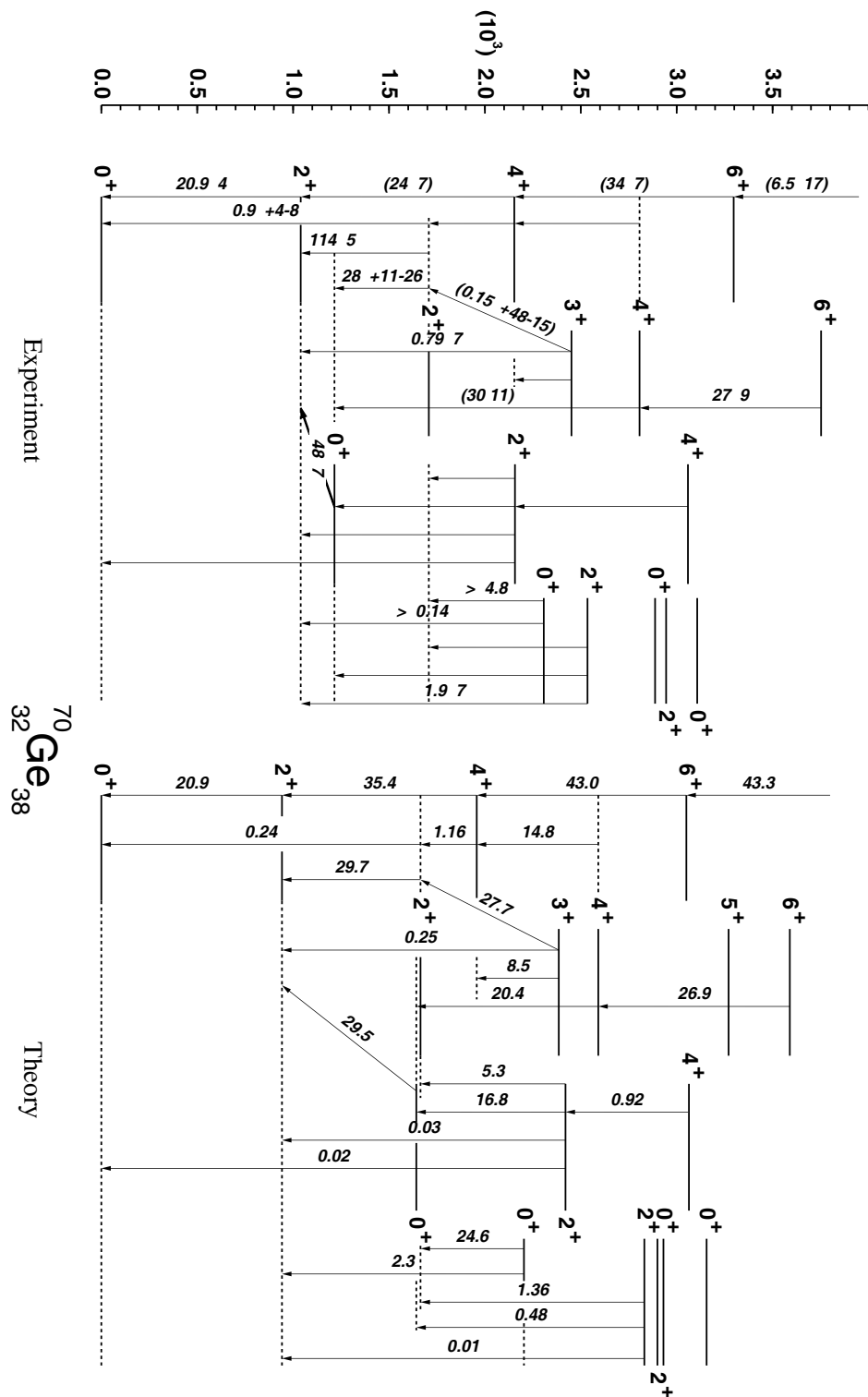


Fig.2. Side-by-side level scheme of ^{70}Ge comparing theoretical to experimental excitation energies and E2 reduced transition probabilities for low-lying, positive parity levels. Energy scale is in MeV. See text for details

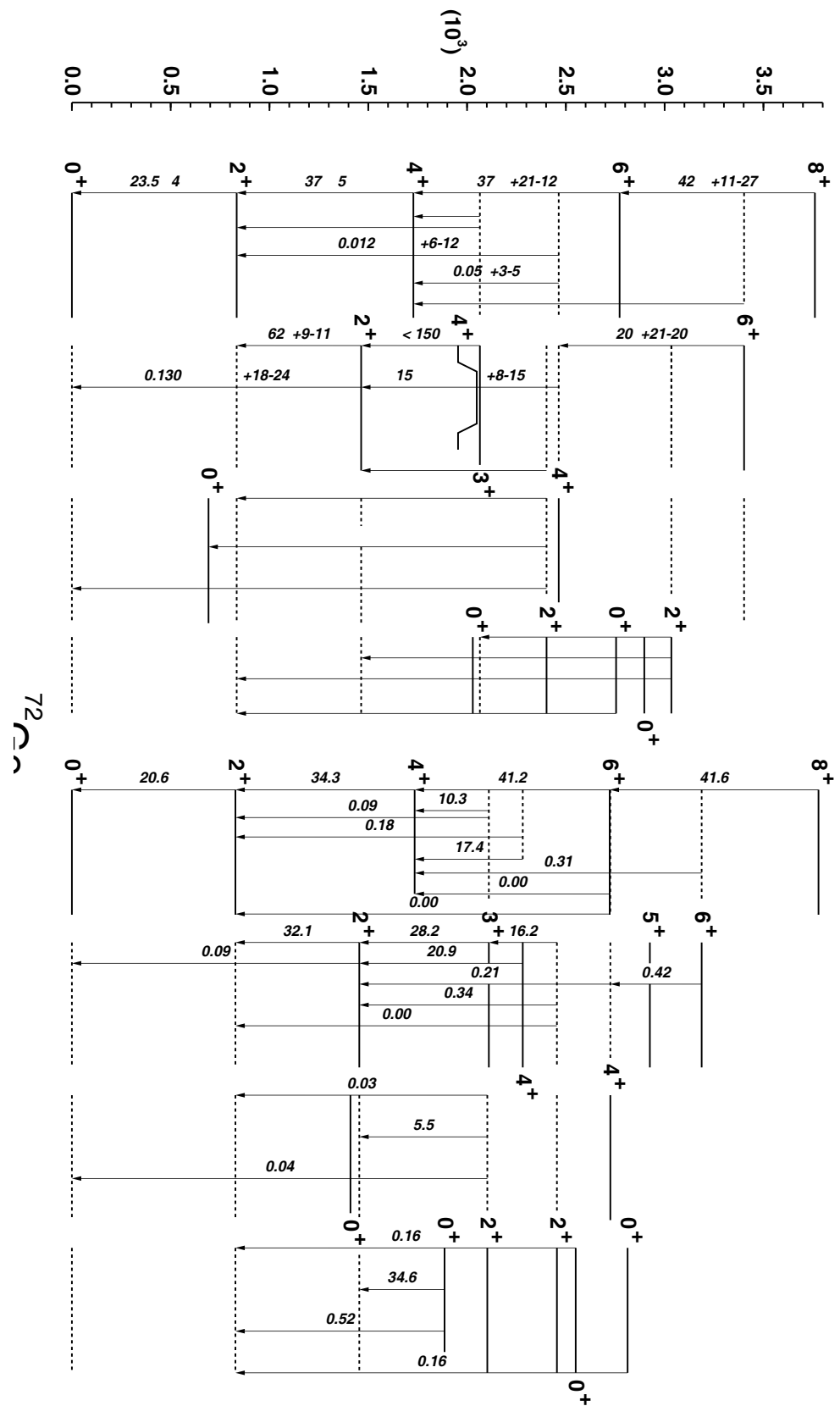


Fig.3. Side-by-side level scheme of ^{72}Ge comparing theoretical to experimental excitation energies and E2 reduced transition probabilities for low-lying, positive parity levels. Energy scale is in MeV. See text for details

4. DCO Ratios Measurements

In fusion-evaporation reactions the compound nucleus is formed in a highly oriented state with its angular momentum in a plane perpendicular to the direction of beam. The evaporation of the particles somewhat disturbs the orientation of states, however, the resulting nucleus maintains a high degree of orientation for a time of the order of 10^{-9} seconds [28].

When such a nucleus emits γ -radiation the relative intensities at different angles depend on the multipolarity of the transition: $I \rightarrow I - 2$ pure quadrupole transitions tend to be emitted more along the beam axis (at 0° and 180°), while $I \rightarrow I - 1$ pure dipole tend to be emitted more perpendicular to it (at 90° and 270°). The distributions are symmetric with respect to the plane perpendicular to the beam axis.

The distribution of γ -ray intensities at any given angle is given by [29]:

$$I(\theta) = \sum_{\ell=even} A_\ell P_\ell(\cos \theta) \quad (2)$$

where $P_\ell(\cos \theta)$ are Legendre polynomials and A_ℓ are the coefficients of the expansion (tabulated in [30]).

Thus, one can distinguish between multipoles by examining the relative γ -ray coincidence intensities at angles approximating 0° and 90° , for example. This method is called DCO (Directional Correlations de-exciting Oriented states) analysis [31]. In our case, the angles used were 143° and 90° . The DCO intensity ratio is defined as:

$$R_{DCO} = \frac{I_{\gamma 2}(143^\circ, 90^\circ) \text{ gated by } \gamma 1(143^\circ, 90^\circ)}{I_{\gamma 2}(90^\circ, 143^\circ) \text{ gated by } \gamma 1(90^\circ, 143^\circ)} \times \varepsilon \quad (3)$$

where $\gamma 1$ is the gating transition, $I_{\gamma 2}$ is the area of the γ -ray transition of interest in the projected spectrum, and ε is the efficiency correction factor.

In this configuration, gating on a stretched quadrupole transition should yield ratios of ≈ 1 for quadrupole transitions and ≈ 0.5 for pure stretched dipole radiation [24].

DCO ratios were measured for 6 transitions in ^{70}Ge and 14 transitions in ^{72}Ge . For those multipolarities that are already known, the measurements match the expected results. We have been able to confirm clearly, through a measured $R_{DCO} = 0.58(14)$, the previously assumed fact that the 1012 keV, $7_1^- \rightarrow 6_1^+$, transition is a pure dipole one (E1).

In Table 2 we present the DCO ratios of transitions visible in ^{70}Ge produced through the $^{12}\text{C} + ^{64}\text{Ni}$ nuclear reaction, gated by the $4_1^+ \rightarrow 2_1^+$, 1113.6 keV transition.

In Table 3 we present the DCO ratios of transitions visible in ^{72}Ge produced through the $^{13}\text{C} + ^{64}\text{Ni}$ nuclear reaction, gated by the $2_1^+ \rightarrow 0_1^+$, 834 keV transition.

Table 2
DCO ratios of transitions measured in ^{70}Ge

E_i [keV]	J_i^π	E_f [keV]	J_f^π	$E\gamma$ [keV]	R_{DCO}	γ -mult. (ref. [15])	γ -mult. (this exp.)
3666.83	6^-	3416.36	5^-	250.57	0.47(13)	M1(+E2)	M1
3955.15	7^-	3666.83	6^-	288.49	0.80(38)	M1(+E2)	M1(+E2)
3058.707	4^+	2156.72	2^+	901.25	1.13(37)	-	E2
4203.7	8^+	3297.06	6^+	906.48	1.34(22)	E2(+M3)	E2(+M3)
1039.485	2^+	0.0	0^+	1039.79	1.05(08)	E2	E2
3297.06	6^+	2153.16	4^+	1144.52	0.78(15)	E2(+M3)	E2(+M3)

Table 3
DCO ratios of transitions measured in ^{72}Ge

E_i [keV]	J_i^π	E_f [keV]	J_f^π	$E\gamma$ [keV]	R_{DCO}	γ -mult. (ref.[20])	γ -mult. (this exp.)
2064.93	3^+	1463.99	2^+	601.37	1.52(45)	M1+E2	M1+E2
3128.86	5^-	2514.79	3^-	614.54	1.32(24)	E2	E2
1463.99	2^+	834.011	2^+	630.41	1.02(14)	M1+E2	E2
3784.18	7^-	3128.86	5^-	655.72	1.33(25)	E2	E2
1728.30	4^+	834.011	2^+	894.54	1.14(10)	E2(+M3)	E2
4741.34	9^-	3784.18	7^-	957.27	1.10(18)	E2	E2
3760.50	8^+	2772.03	6^+	988.92	0.69(09)	E2	E2
3784.18	7^-	2772.03	6^+	1012.41	0.58(14)	-	E1
3080.34	4^+	2064.93	3^+	1015.89	1.44(43)	-	M1+E2
2772.03	6^+	1728.30	4^+	1044.18	1.06(10)	E2	E2
2514.79	4^+	1463.99	2^+	1050.68	0.79(19)	E1+M2	E1+M2
4820.0	10^+	3760.50	8^+	1059.74	0.94(05)	E2	E2
5837.8	11^-	4741.34	9^-	1096.62	1.09(24)	E2	E2
3898.48	7^-	2772.03	6^+	1127.22	0.72(22)	-	E1

5. Conclusions

We have performed a successful experiment in IFIN-HH in which we investigated experimentally some of the less favored channels of the $^{12}\text{C} + ^{64}\text{Ni}$

and $^{13}\text{C} + ^{64}\text{Ni}$ nuclear reactions, namely $^{64}\text{Ni}(^{12}\text{C}, \alpha 2n\gamma)^{70}\text{Ge}$, $^{64}\text{Ni}(^{12}\text{C}, \alpha\gamma)^{70}\text{Ge}$, $^{64}\text{Ni}(^{13}\text{C}, \alpha 3n\gamma)^{70}\text{Ge}$, and $^{64}\text{Ni}(^{13}\text{C}, \alpha n\gamma)^{72}\text{Ge}$. Calculations were performed within the IBA-1 model framework, and the results turned out in good agreement with known experimental data. DCO ratios were measured for 6 transitions in ^{70}Ge and 14 transitions in ^{72}Ge . For those multipolarities that are already known, the measurements match the expected results. We have been able to confirm clearly, through a measured $R_{DCO} = 0.58(14)$, the previously assumed fact that the 1012 keV, $7_1^- \rightarrow 6_1^+$, transition is a pure dipole one (E1).

6. Acknowledgments

G. Drafta acknowledges financial support through the contract POSDRU/6/1.5/S/16.

R E F E R E N C E S

- [1] *W. Nazarewicz et al.* Nucl. Phys. **A435**(1985)397
- [2] *D. Pantelică et al.* Phys. Rev. C **82**, 044313 (2010)
- [3] *J. H. Hamilton*, Treatise on Heavy Ion Science, Vol. 8, edited by D. A. Bromley (Plenum, New York, 1989), p. 3.
- [4] *Nuclear Structure of the Zirconium Region*, edited by J. Eberth, R. A. Mayer, and K. Sistemich (Springer Verlag, Berlin, 1988), p. 17.
- [5] *M. Carchidi et al.* Phys. Rev. C **30**, 1293 (1984).
- [6] *H. T. Fortune et al.* Phys. Rev. C **36**, 2584 (1987).
- [7] *M. Sugawara et al.* Eur. Phys. J. A **16**, 409 (2003).
- [8] *B. Kotliński et al.* Nucl. Phys. **A519**, 646 (1990).
- [9] *Y. Toh et al.* Eur. Phys. J. A **9**, 353 (2000).
- [10] *Y. Toh et al.*, J. Phys. G: Nucl. Part. Phys. **27**, 1475 (2001).
- [11] *C. Morand et al.* Phys. Rev. C **13**, 2182 (1976).
- [12] *R. L. Robinson et al.* Phys. Rev. C **16**, 2268 (1977).
- [13] *B. Mukherjee et al.*, Acta Phys. Hung. N. S. **11**, 189 (2000).
- [14] *M. Sugawara et al.* Phys. Rev. C **81**, 024309 (2010)
- [15] *J. K. Tuli*, Nuclear Data Sheets **103**, 389 (2004)
- [16] *K. J. Weeks et al.*, Phys. Rev. C **24**, 703 (1981).024309-9
- [17] *P. D. Duval et al.*, Phys. Lett. **B124**, 297 (1983)
- [18] *A. Petrovici et al.*, Nucl. Phys. **A483**, 317 (1988).
- [19] *C. Morand et al.*, Nucl.Phys. **A313**, 45 (1979)
- [20] *D. Abriola, A.A. Sonzogni*, Nuclear Data Sheets **111**, 1 (2010)
- [21] *S. Dobrescu et al.*, AIP CONFERENCE PROCEEDINGS, **1099**, 51-54 (2009)
- [22] *F. Pühlhofer*, Nucl. Phys. **A280** 267 (1977)
- [23] *O. B. Tarasov, D. Bazin*, Nucl. Instr. and Meth. B(204), 174-178 (2003)
- [24] *N. Mărginean*, private communication
- [25] *R. F. Casten, D. D. Warner*, Rev. Mod. Phys. **C 60**, 389 (1988).
- [26] *F. Iachello, A. Arima*, The Interacting Boson Model (Cambridge University Press, Cambridge, 1987).

- [27] *O. Scholten*, program packages PHINT and FBEM (unpublished).
- [28] *Gerda Neyens*, Rep. Prog. Phys., **66**, 633-689 (2003)
- [29] *K. Siegbahn* (Ed), Alpha-, Beta- and Gamma-Ray Spectroscopy, North-Holland (1965)
- [30] *E. der Mateosian and A.W. Sunyar*, At. Data and Nucl. Data Tables **13** 391, 407 (1974)
- [31] *K.S. Krane et al.*, Nucl. Data Tables **11** 351 (1973)